International Journal of Innovative Computing, Information and Control
Volume **9**, Number **7**, July **2013**

ICIC International ©2013 ISSN 1349-4198
pp. 2727–2740

DSP IMPLEMENTATION OF SPEED VECTOR CONTROL FOR SINGLE-PHASE INDUCTION MOTOR BASED ON PROPORTIONAL SLIDING MODE CONTROL LAW

Noureddaher Zaidi[1], Hechmi Ben Azza[1], Mohamed Jemli[1]
Mohamed Boussak[2] and Abdelkader Chaari[1]

[1]Unité de Recherche en Commande, Surveillance et Sûreté de Fonctionnement des Systèmes (C3S)
Ecole Supérieure des Sciences et Techniques de Tunis (ESSTT)
5, Avenue Taha Hussein, BP 56, Bab Mnara 1008 Tunis, Tunisia
zaidi.nour@unite-c3s.com; benazzahechmi@voila.fr
mohamed.jemli@isetr.rnu.tn; nabile.chaari@yahoo.fr

[2]Laboratoire des Sciences de l'Information et des Systèmes (LSIS), CNRS UMR 6168
Centrale Marseille Recherche et Technologies (CMRT)
Ecole Centrale Marseille (ECM), Technopôle Château Gombert, 13451 Marseille Cedex 20, France
mboussak@centrale-marseille.fr

Received March 2012; revised July 2012

Abstract. *The accuracy knowledge of some state variables and motor parameters is required to the design of an efficient decoupled block or an exact linearization step dedicated for the classical Field Oriented Control (FOC) strategies. The aim of this paper is the elaboration of FOC strategy with high tracking performances and free of the on line adjustable decoupled block to drive a Single-Phase Induction Motor (SPIM). A full digital implementation of a novel speed vector control strategy based on Sliding Mode Control (SMC), to drive a SPIM, is presented. Adopting a very simple sliding surface design, and with the aim to generate a control signal free of chattering, three controllers qualified as Proportional Sliding Mode Controller (PSMC) are investigated. Adaptive sliding gain is conceived to improve the speed trajectory tracking performances under load disturbances. The asymptotically stability of the adaptive sliding mode control system is proved by means of the Lyapunov stability approach. An experimental platform around a DSP (dSPACE DS1104) is conceived to evaluate the real time implementation and the performances of the proposed speed vector control strategy. Simulation and experimental results highlight the effectiveness of the presented scheme and the performances of the adopted control law.*

Keywords: Sliding mode control, Chattering, Single-phase induction motor, Indirect rotor field-oriented control, DSP implementation

1. **Introduction.** The Single-Phase Induction Motor (SPIM) is usually used for consumer fixed-speed applications such as in blowers, compressors, fans, refrigerators, washing machines, conveyors, machine tools, pumps, freezers and residential devices such as a wide variety of HVAC (Heating, Ventilation and Air-Conditioning). Under most advantageous conditions, the SPIM efficiency is typically low (less than 50%) [1-4]. Approximately 10% of the total electricity used in all kinds of motors is consumed by the SPIM [1]. It is predictable in [1] that 1.7 billion KWh/year of energy is saved if the efficiency of SPIM increases by only 1%. Motivated by the considerable cost reduction the use of the variable speed drives (VSDs) is one of the most effective technical ways to save a great deal of energy, money for consumers and increase the motor efficiency [5-7]. Therefore, this is a current topic of research interest. A number of works have reported the improvement of SPIM efficiency up to now. The research interested in the SPIM aimed essentially to

reduce the energy consumption via the improvement of the electromagnetic torque quality for fixed speed and VSDs [4,8].

The classical technique firstly invented for the induction motor control and secondly applied to SPIM control, is the field-oriented control. This technique needs a partial feedback linearization [9] or a decoupled block [10,11], for applying linear control method such as PID controller. Moreover, the performances of field-oriented control strategy depend on the accuracy knowledge of some states variables and parameters. Previous analysis has shown that in the case of the SPIM it is necessary to look for new controller structures that offer better disturbance rejection properties [12]. Many controller structures have been proposed during the last years to drive the SPIM. In [8,11] classical PI controllers are integrated in Indirect Rotor Field Oriented Control (IRFOC) strategy to drive a SPIM. In [12] the authors employ two different synchronous controllers: the positive-sequence synchronous controller is designed to compensate the direct sequence term and the negative-sequence synchronous controller is designed to compensate the inverse-sequence term. Despite their good performances, this technique requires the use of four controllers and the same number of coordinate transformation which can consequently affect the cost of real time implementation. Recently, a diametrical inversion of the stator voltages associated with a sliding mode controller was proposed to implement a speed controller for SPIM in [13]. This method is easy to implement but it generates non neglect currents and torque oscillations.

It is well known that the Sliding Mode Control (SMC) technique offers fast response and good transient performances for a wide operating range as compared with the conventional linear methods. Moreover, it was particularly utilized thanks to its ability to deal with nonlinearities and its robust behavior against parameters uncertainties and external disturbances [14-16]. However, the chattering phenomenon is the main obstacle encountered in real time applications of SMC technique. In order to generate a control law free of chattering or at least with lower oscillations effects, many techniques are used [17-20]. The most popular ones are the low pass filter and the approximation of the signum function by a smoother continuous one [17-20]. Thus, we propose a new IRFOC strategy without resort to the decoupled block or the linearization step to drive a SPIM. The proposed strategy includes the design of three high performances Proportional Sliding Mode Controllers (PSMC); one is reserved to control the SPIM speed and the two others are dedicated to controlling the stator currents. The speed PSMC incorporates an adaptive sliding gain to improve the trajectory tracking performance. To attain the prospective of SMC technique and to reduce the chattering effect, the last technique is utilized inside the adaptive sliding gain. The stability of the PSMCs is proved by using the Lyapunov approach. In addition, the suitable values of the switching gains ensuring sliding mode to occur and achieving the control objectives will be determined from the obvious-stability study. So that, we can avoid undesirable oscillations of the system responses, caused by a bad choice of the switching gains when they are fixed to the maximum value of the control effort for simplicity reasons [16].

The paper is organized as follows. Section 2 presents the SPIM dynamic model and the proposed IRFOC strategy. Section 3 briefly reviews the SMC theory and deals with the speed and the currents sliding mode controllers design. The developed prototype used for the experimental test followed by simulation and experimental results is presented and discussed in Section 4. Finally, some concluding remarks are drawn in Section 5.

2. **Indirect Field Oriented Control.**

2.1. **SPIM symmetrical model.** The dynamic model of the SPIM in a stationary reference frame can be described as follows:

– Stator voltages:

$$\begin{bmatrix} v_{s\alpha} \\ v_{s\beta} \end{bmatrix} = \begin{bmatrix} R_{sd} & 0 \\ 0 & R_{sq} \end{bmatrix} \begin{bmatrix} i_{s\alpha} \\ i_{s\beta} \end{bmatrix} + \begin{bmatrix} p & 0 \\ 0 & p \end{bmatrix} \begin{bmatrix} \varphi_{s\alpha} \\ \varphi_{s\beta} \end{bmatrix} \tag{1}$$

– Rotor voltages:

$$\begin{bmatrix} 0 \\ 0 \end{bmatrix} = \begin{bmatrix} R_r & 0 \\ 0 & R_r \end{bmatrix} \begin{bmatrix} i_{r\alpha} \\ i_{r\beta} \end{bmatrix} + \begin{bmatrix} p & \omega_r \\ -\omega_r & p \end{bmatrix} \begin{bmatrix} \varphi_{r\alpha} \\ \varphi_{r\beta} \end{bmatrix} \tag{2}$$

– Stator flux:

$$\begin{bmatrix} \varphi_{s\alpha} \\ \varphi_{s\beta} \end{bmatrix} = \begin{bmatrix} L_{sd} & 0 \\ 0 & L_{sq} \end{bmatrix} \begin{bmatrix} i_{s\alpha} \\ i_{s\beta} \end{bmatrix} + \begin{bmatrix} M_{srd} & 0 \\ 0 & M_{srq} \end{bmatrix} \begin{bmatrix} i_{r\alpha} \\ i_{r\beta} \end{bmatrix} \tag{3}$$

– Rotor flux:

$$\begin{bmatrix} \varphi_{r\alpha} \\ \varphi_{r\beta} \end{bmatrix} = \begin{bmatrix} L_r & 0 \\ 0 & L_r \end{bmatrix} \begin{bmatrix} i_{r\alpha} \\ i_{r\beta} \end{bmatrix} + \begin{bmatrix} M_{srd} & 0 \\ 0 & M_{srq} \end{bmatrix} \begin{bmatrix} i_{s\alpha} \\ i_{s\beta} \end{bmatrix} \tag{4}$$

– Mechanical equation:

$$J\frac{d\omega_r}{dt} + f\omega_r = n_p(T_e - T_L) \tag{5}$$

– Electromagnetic torque:

$$T_e = n_p(M_{srq} i_{s\beta} i_{r\alpha} - M_{srd} i_{s\alpha} i_{r\beta}) \tag{6}$$

Due to the reality that the main and auxiliary stator windings present unequal stator resistances and inductances, this model is qualified as asymmetrical. In order to apply the IRFOC strategy for a SPIM, a symmetrical model must be established and variables transformation is requisite. The following stator variables transformation T proposed in [12] is adopted.

$$T = \begin{bmatrix} 1 & 0 \\ 0 & K \end{bmatrix}; \quad K = \frac{M_{srd}}{M_{srq}} \tag{7}$$

where the new stator variables are given by:

$$\begin{bmatrix} i_{s\alpha} \\ i_{s\beta} \end{bmatrix} = T \begin{bmatrix} i_{s\alpha 1} \\ i_{s\beta 1} \end{bmatrix}; \begin{bmatrix} v_{s\alpha} \\ v_{s\beta} \end{bmatrix} = T^{-1} \begin{bmatrix} v_{s\alpha 1} \\ v_{s\beta 1} \end{bmatrix} \text{ and } \begin{bmatrix} \varphi_{s\alpha} \\ \varphi_{s\beta} \end{bmatrix} = T^{-1} \begin{bmatrix} \varphi_{s\alpha 1} \\ \varphi_{s\beta 1} \end{bmatrix} \tag{8}$$

Substituting, the new stator variables in (1)-(4), we obtain:

$$\begin{bmatrix} v_{s\alpha 1} \\ v_{s\beta 1} \end{bmatrix} = \begin{bmatrix} R_{sd} & 0 \\ 0 & R_{sd} \end{bmatrix} \begin{bmatrix} i_{s\alpha 1} \\ i_{s\beta 1} \end{bmatrix} + \begin{bmatrix} p & 0 \\ 0 & p \end{bmatrix} \begin{bmatrix} \varphi_{s\alpha 1} \\ \varphi_{s\beta 1} \end{bmatrix} + \begin{bmatrix} 0 \\ K^2 R_{sq} - R_{sd} \end{bmatrix} \begin{bmatrix} i_{s\alpha 1} \\ i_{s\beta 1} \end{bmatrix} \tag{9}$$

$$\begin{bmatrix} 0 \\ 0 \end{bmatrix} = \begin{bmatrix} R_r & 0 \\ 0 & R_r \end{bmatrix} \begin{bmatrix} i_{r\alpha} \\ i_{r\beta} \end{bmatrix} + \begin{bmatrix} p & \omega \\ -\omega & p \end{bmatrix} \begin{bmatrix} \varphi_{r\alpha} \\ \varphi_{r\beta} \end{bmatrix} \tag{10}$$

$$\begin{bmatrix} \varphi_{s\alpha 1} \\ \varphi_{s\beta 1} \end{bmatrix} = \begin{bmatrix} L_{sd} & 0 \\ 0 & L_{sd} \end{bmatrix} \begin{bmatrix} i_{s\alpha 1} \\ i_{s\beta 1} \end{bmatrix} + \begin{bmatrix} M_{srd} & 0 \\ 0 & M_{srd} \end{bmatrix} \begin{bmatrix} i_{r\alpha} \\ i_{r\beta} \end{bmatrix} + \begin{bmatrix} 0 \\ K^2 L_{sq} - L_{sd} \end{bmatrix} \begin{bmatrix} i_{s\alpha 1} \\ i_{s\beta 1} \end{bmatrix} \tag{11}$$

$$\begin{bmatrix} \varphi_{r\alpha} \\ \varphi_{r\beta} \end{bmatrix} = \begin{bmatrix} L_r & 0 \\ 0 & L_r \end{bmatrix} \begin{bmatrix} i_{r\alpha} \\ i_{r\beta} \end{bmatrix} + \begin{bmatrix} M_{srd} & 0 \\ 0 & M_{srd} \end{bmatrix} \begin{bmatrix} i_{s\alpha 1} \\ i_{s\beta 1} \end{bmatrix} \tag{12}$$

The set of Equations (9)-(12) besides the mechanical Equation (5) represents the symmetrical model of the SPIM in stationary reference frame; therefore, the field-oriented approach can be applied.

2.2. **IRFOC strategy.** The main idea behind the field-oriented strategy is to align the flux vector along a chosen direction so that the behaviours of the SPIM look as a DC motor behaviours', where the flux and the torque can be controlled independently by the direct and quadratic currents. The first derivative rotor flux form can be obtained by the substitution of (12) in (10):

$$p\begin{bmatrix}\varphi_{r\alpha}\\ \varphi_{r\beta}\end{bmatrix}=\begin{bmatrix}-\frac{1}{T_r} & -\omega_r\\ \omega_r & -\frac{1}{T_r}\end{bmatrix}\begin{bmatrix}\varphi_{r\alpha}\\ \varphi_{r\beta}\end{bmatrix}+\begin{bmatrix}\frac{M_{srd}}{T_r} & 0\\ 0 & \frac{M_{srd}}{T_r}\end{bmatrix}\begin{bmatrix}i_{s\alpha 1}\\ i_{s\beta 1}\end{bmatrix} \tag{13}$$

wherein T_r represents the rotor constant time.

Using the synchronous transformation T_s, this form can be transformed in synchronous reference frame (denoted by the superscript d, q) as:

$$p\begin{bmatrix}\varphi_{rd}\\ \varphi_{rq}\end{bmatrix}=\begin{bmatrix}-\frac{1}{T_r} & \omega_{sl}\\ -\omega_{sl} & -\frac{1}{T_r}\end{bmatrix}\begin{bmatrix}\varphi_{rd}\\ \varphi_{rq}\end{bmatrix}+\begin{bmatrix}\frac{M_{srd}}{T_r} & 0\\ 0 & \frac{M_{srd}}{T_r}\end{bmatrix}\begin{bmatrix}i_{sd1}\\ i_{sq1}\end{bmatrix} \tag{14}$$

where:

$$\begin{bmatrix}\varphi_{rd}\\ \varphi_{rq}\end{bmatrix}=T_s\begin{bmatrix}\varphi_{r\alpha}\\ \varphi_{r\beta}\end{bmatrix};\ \begin{bmatrix}i_{sd1}\\ i_{sq1}\end{bmatrix}=T_s\begin{bmatrix}i_{s\alpha 1}\\ i_{s\beta 1}\end{bmatrix};\ T_s=e^{j\theta_s}\text{ and }\omega_{sl}=\omega_s-\omega_r \tag{15}$$

Since the d-axis of the reference frame is oriented along the rotor flux vector, rotor flux components become:

$$\varphi_{rd}=\varphi_r;\quad \varphi_{rq}=0 \tag{16}$$

Therefore, we get the following fundamental expressions of oriented flux control from which the direct and quadratic reference currents i_{sd}^*, i_{sq}^* and slip frequency ω_{sl}^* are carried out:

$$p\varphi_r^*=-\frac{1}{T_r}\varphi_r^*+\frac{M_{srd}}{T_r}i_{sd1}^* \tag{17}$$

$$\omega_{sl}^*=\frac{M_{srd}}{T_r\varphi_r^*}i_{sq1}^* \tag{18}$$

$$T_e=n_p\frac{M_{srd}}{L_r}\varphi_r^*i_{sq1}^* \tag{19}$$

According to (15), (16) and the fact that $(K^2L_{sq}-L_{sd}\cong 0)$, the stator voltage commands can be expressed, in synchronous rotating reference frame as:

$$\begin{aligned}\begin{bmatrix}v_{sd1}\\ v_{sq1}\end{bmatrix}=&\begin{bmatrix}R_{sd}+\frac{M_{srd}^2}{T_rL_r} & \omega_sL_{sd}\sigma_{sd}\\ -\omega_sL_{sd}\sigma_{sd} & K^2R_{sq}+\frac{M_{srd}^2}{T_rL_r}\end{bmatrix}\begin{bmatrix}i_{sd1}\\ i_{sq1}\end{bmatrix}\\ &+\begin{bmatrix}L_{sd}\sigma_{sd} & 0\\ 0 & L_{sd}\sigma_{sd}\end{bmatrix}p\begin{bmatrix}i_{sd1}\\ i_{sq1}\end{bmatrix}+\begin{bmatrix}-\frac{M_{srd}}{L_rT_r}\varphi_r\\ \frac{M_{srd}}{L_r}\omega\varphi_r\end{bmatrix}\end{aligned} \tag{20}$$

Figure 1 presents the block diagram of the ameliorated IRFOC strategy. In addition to the control model, it involves three sliding mode controllers. Two of them are designed to control the main and auxiliary windings currents, while the next one permits to drive the SPIM speed. An appropriate design of the currents controllers, permit us to overcome the compensative block, usually utilised with the conventional controllers.

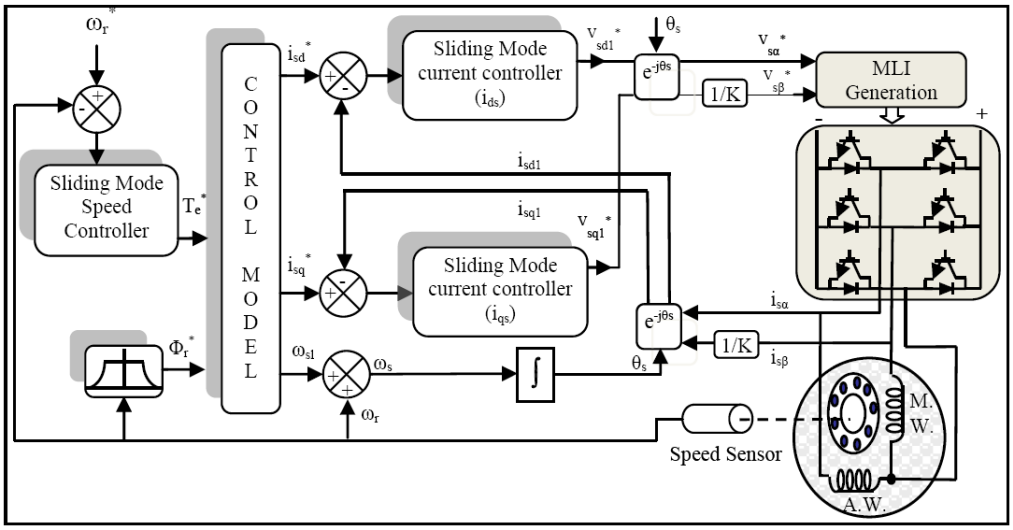

FIGURE 1. Block diagram of ameliorated IRFOC strategy

3. **Sliding Mode Control Design.** SMC is a technique derived from variable structure control originally introduced by Utkin [19]. The goal of the SMC is to find a Sliding Surface (SS) and a control law, so that the system states will reach the SS in a finite time and reside on it. So, the design of such control involves two steps [9,21]. The first one is mainly reserved to the choice of an SS which provides the desired behaviour when the system dynamics reach the sliding mode. In the second step, an appropriate control law is elaborated; which will force the system state trajectories to reach the SS and stay there. In order to accomplish this goal, a reaching condition must be fulfilled [17,21]. This condition driven from Lyapunov stability theory is expressed by:

$$\dot{V} = S\dot{S} \leq 0 \tag{21}$$

where V and S are respectively a candidate Lyapunov function and a switching function.

In order to ensure a finite time convergence to the SS, this condition is often replaced by:

$$\dot{V} = S\dot{S} \leq -\eta\,|S|\,; \quad \eta > 0 \tag{22}$$

Furthermore, Equation (22) implies that some dynamic uncertainties or disturbances can be tolerated while the states stay in the SS. The required reaching time (t_r) to the SS, starting from initial condition $S(0)$, is bounded by:

$$t_r \leq \frac{|S(0)|}{\eta} \tag{23}$$

The control law U is usually composed of two terms:

$$U = U_{eq} + U_n \tag{24}$$

The first term U_{eq} is the so-called equivalent control law, calculated from the choice of the sliding mode dynamics. The second term U_n is the non-linear control law, designed around the basic form expressed by:

$$U_n = K\text{sign}(S) \tag{25}$$

This term is carried out respecting the reaching condition and explains the control nature. At the same time, this term takes care of the uncertainties and makes certain that the states will be governed towards the SS.

The sliding surfaces, used to elaborate the different control schemes presented in this work, are based on the simple tracking error expression. This choice is justified by the simplicity of the required analysis and by the fact that the errors will be cancelled if the SSs are attained and maintained.

3.1. **Current sliding mode controllers design.** Let us consider the following switching functions (S_d and S_q):

$$\begin{bmatrix} S_d \\ S_q \end{bmatrix} = \begin{bmatrix} c_d e_d \\ c_q e_q \end{bmatrix} \text{ where } \begin{bmatrix} e_d \\ e_q \end{bmatrix} = \begin{bmatrix} i^*_{sd1} - i_{sd1} \\ i^*_{sq1} - i_{sq1} \end{bmatrix} \text{ and } c_d, c_q > 0 \tag{26}$$

If the main and auxiliary windings currents reach the switching functions and stay there, then their errors will be cancelled and they tend to the desired values. This can be expressed as:

$$\begin{bmatrix} \dot{S}_d \\ \dot{S}_q \end{bmatrix} = \begin{bmatrix} S_d \\ S_q \end{bmatrix} = \begin{bmatrix} 0 \\ 0 \end{bmatrix} \Rightarrow \begin{bmatrix} i_{sd1} = i^*_{sd1} \\ i_{sq1} = i^*_{sq1} \end{bmatrix} \tag{27}$$

Expression (20) can be arranged (considering (17), (18) and (27)) as follows:

$$\begin{aligned} p \begin{bmatrix} i_{sd1} \\ i_{sq1} \end{bmatrix} = & - \frac{1}{L_{sd}\sigma_{sd}} \begin{bmatrix} R_{sd} + \frac{M^2_{srd}}{T_r L_r} & 0 \\ 0 & K^2 R_{sq} + \frac{M^2_{srd}}{T_r L_r} \end{bmatrix} \begin{bmatrix} i_{sd1} \\ i_{sq1} \end{bmatrix} \\ & + \frac{1}{L_{sd}\sigma_{sd}} \begin{bmatrix} v_{sd1} \\ v_{sq1} \end{bmatrix} + \begin{bmatrix} G_d \\ G_q \end{bmatrix} \end{aligned} \tag{28}$$

where the decoupled terms G_d and G_q are given by:

$$\begin{bmatrix} G_d \\ G_q \end{bmatrix} = \begin{bmatrix} -\omega_s i_{sq1} + \frac{M_{srd}}{L_r T_r L_{sd}\sigma_{sd}} \varphi_r \\ \omega_s i_{sd1} - \frac{M_{srd}}{L_r L_{sd}\sigma_{sd}} \omega \varphi_r \end{bmatrix} \tag{29}$$

As mentioned at the precedent paragraph, we propose the control law made by the combination of equivalent term and nonlinear term. The expression of the equivalent control (30) can be obtained from Equation (28), and under the conditions expressed by (27).

$$\begin{bmatrix} V_{sd1eq} \\ V_{sq1eq} \end{bmatrix} = L_{sd}\sigma_{sd} \begin{bmatrix} \left(R_{sd} + \frac{M^2_{srd}}{T_r L_r}\right) i^*_{sd1} + \frac{d}{dt} i^*_{sd1} \\ \left(K^2 R_{sq} + \frac{M^2_{srd}}{T_r L_r}\right) i^*_{sq1} + \frac{d}{dt} i^*_{sq1} \end{bmatrix} \tag{30}$$

where the proposed nonlinear term is given by:

$$U_n = \begin{bmatrix} U_d \\ U_q \end{bmatrix} = \begin{bmatrix} K_d \text{sign}(S_d) - G_d L_{sd}\sigma_{sd} \\ K_q \text{sign}(S_q) - G_q L_{sd}\sigma_{sd} \end{bmatrix} \tag{31}$$

Indeed, we consider the following candidate Lyapunov functions:

$$\begin{bmatrix} V_d \\ V_q \end{bmatrix} = \begin{bmatrix} \frac{1}{2} S_d^2 \\ \frac{1}{2} S_q^2 \end{bmatrix} \tag{32}$$

The switching gains K_d and K_q must be calculated satisfying the reaching condition (22). This means that:

$$\begin{bmatrix} \text{sign}(S_d)\dot{S}_d \\ \text{sign}(S_q)\dot{S}_q \end{bmatrix} \leq \begin{bmatrix} \eta_d \\ \eta_q \end{bmatrix} \tag{33}$$

where η_d and η_q are positives reels chosen according to the desired SS currents reaching times. Moreover, the currents switching functions are reached in finite times (t_{dr}, t_{qr}) bounded as:

$$t_{rd} \leq \frac{|S_d(0)|}{\eta_d} \text{ and } t_{rq} \leq \frac{|S_q(0)|}{\eta_q} \tag{34}$$

Arranging ((28)-(31) and (33)), we get:

$$\begin{bmatrix} L_{sd}\sigma_{sd}\frac{\eta_d}{c_d} - \frac{R_{sd}}{c_d}|S_d| \\ L_{sd}\sigma_{sd}\frac{\eta_q}{c_q} - \frac{K^2 R_{sq}}{c_q}|S_q| \end{bmatrix} \leq \begin{bmatrix} K_d \\ K_q \end{bmatrix} \tag{35}$$

Equation (35) must be verified some are the value of switching functions, so we adopted the following inferior limit gains:

$$\begin{bmatrix} L_{sd}\sigma_{sd}\frac{\eta_d}{c_d} \\ L_{sd}\sigma_{sd}\frac{\eta_q}{c_q} \end{bmatrix} \leq \begin{bmatrix} K_d \\ K_q \end{bmatrix} \tag{36}$$

The on line adjustable decoupled terms G_d and G_q can be replaced by a fixed nominal terms. This substitution is only possible when the considered instantly state variables are equal to their references values. Such condition is guaranteed during the entire sliding phase. While in reaching phase, the difference between terms will be regarded as external disturbances and will be implicitly recovered by the non-linear control law terms.

Thus, the designed PSMCs do not necessitate a decoupled block as well as accuracy knowledge of their terms to compensate the effect of the coupled terms G_d and G_q as in the case of conventional controllers.

3.2. **Speed sliding mode controller design.** The same approach is utilised to synthesize the SM speed controller. So, let us consider the following switching function S_ω:

$$S_\omega = c_\omega e_\omega \text{ where } e_\omega = \omega_r^* - \omega_r \text{ and } c_\omega > 0 \tag{37}$$

If the switching function is reached and the system still with, then the error will be cancelled and the speed will tend to the reference. As the precedent paragraph, we propose the same control law form composed by two terms: equivalent and discontinue control terms (Equation (24)). Under the conditions expressed by (38), the expression of the equivalent control (39) can be obtained from mechanical equation.

$$S_\omega = \dot{S}_\omega = 0 \text{ and } T_L = 0 \tag{38}$$

$$U_{\omega eq} = \frac{1}{n_p}\left[J\frac{d}{dt}\omega^* + f\omega^*\right] \tag{39}$$

Adopting the same candidate Lyapunov function form as (21) and using the Lyapunov stability approach, we get the inferior limit gain K_ω of the discontinue control term U_ω:

$$K_\omega \geq \frac{J}{c_\omega}\eta_\omega + n_p\,|T_{L\max}| \tag{40}$$

For a desired speed reaching time $t_{r\omega}$, the inferior limit gain is:

$$K_\omega \geq \frac{J}{t_{r\omega}}\omega_r^* + n_p\,|T_{L\max}| \tag{41}$$

Expressions (40) and (41) are independents of motor parameters (except the inertia which remains constant in our case), so the developed speed PSMC maneuvers in robust mode against eventual motor parameters variation. In order to improve the trajectory tracking performance and make the SS more attractive, we are going to adopt a speed PSMC law U_ω that incorporates an adaptive sliding gain mechanism as follows:

$$U_\omega = U_{\omega eq} + K_\omega(1 + \xi\,|S_\omega|)\text{sign}(S_\omega) \tag{42}$$

where ξ is a positive constant that permits us to ameliorate the reaching time from an initial condition.

As shown in Figure 1, the output of the speed regulator represents the torque reference. So, in order to generate a reference value free or at least with lower oscillations effects

of chattering the approximation of the signum function by a smoother continuous one is utilized. This approximated function is given by the following form:

$$\text{sign}(S_\omega) = \frac{S_\omega}{|S_\omega| + \delta} \text{ where } \varepsilon \geq \delta > 0 \tag{43}$$

4. Simulation and Experimental Results.

4.1. Experimental setup presentation.

In order to validate the novel IRFOC strategy of the SPIM and to verify SM controllers' performances, a laboratory stand was developed. Figure 2 illustrates the adopted experimental setup synoptic and gives the most important materials utilized. A photograph of this experimental prototype is shown in Figure 3, where, the SPIM is supplied by three-leg voltage source inverter, through six bipolar transistors. Two legs are dedicated for the control of the main and auxiliary windings voltages and the third one is used for the control of the offset voltage. The connection topology of the main and auxiliary windings to the three-leg inverter is also shown. The load torque is applied via a magnetic powder brake coupled to the SPIM.

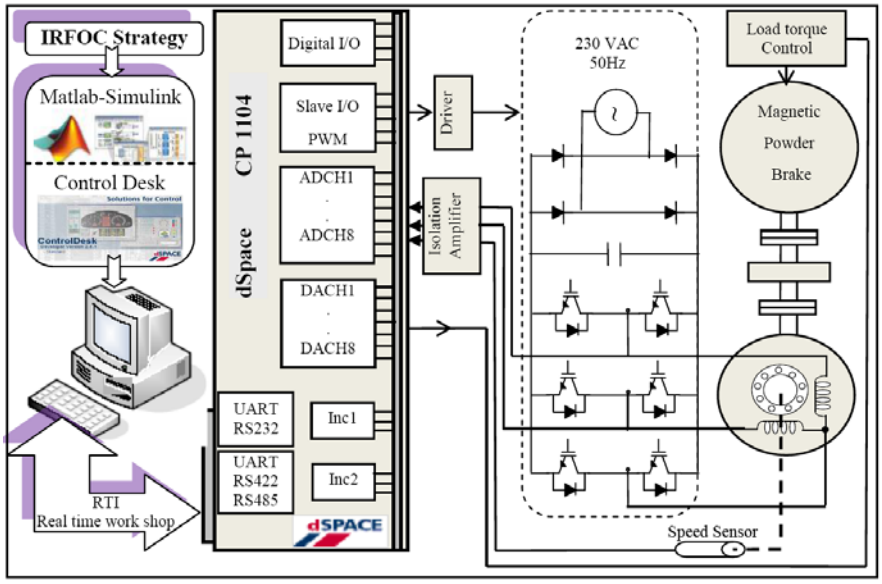

FIGURE 2. Experimental setup

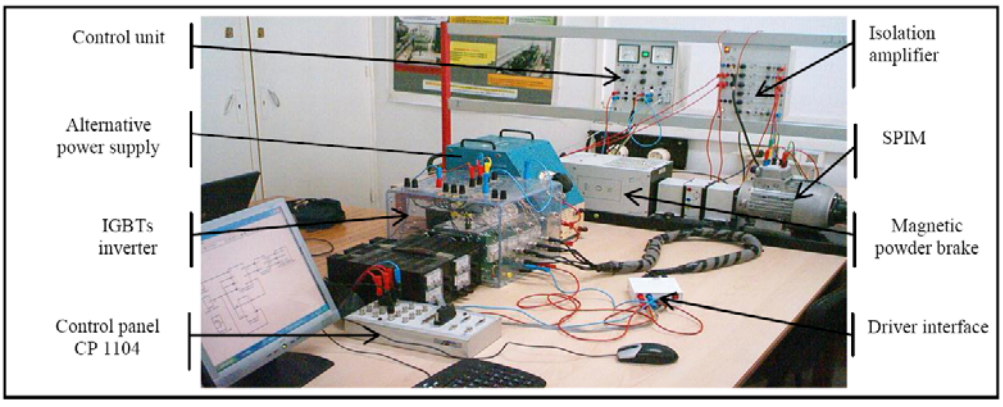

FIGURE 3. Experimental setup photograph

The experimentation was achieved using MATLAB Simulink and dSPACE DS1104 real-time controller board. This board incorporates a Motorola Power PC 603e model, which operates at a frequency of 250 MHz, and a Digital Signal Processing (TMS320F240-20 MHz). In this experimentation, we adopted a sinusoidal PWM technique to generate the PWM signals with a switching frequency of 3 kHz and a dead time of 2 μs for the three-leg inverter as follows:

– Leg 1 PWM duty cycle: calculated with respect to the direct control voltage $V_{s\alpha ref}$.

– Leg 2 PWM duty cycle: calculated with respect to the quadratic control voltage $V_{s\beta ref}$.

– Leg 3 PWM duty cycle: kept constant equal to 0.5 to supply a zero reference voltage.

The sampling time of the control algorithm is of 60 μs.

The used SPIM parameters are detailed in Table 1, where the SM speed controller and the SM d-q axis currents controller parameters are listed in Table 2.

TABLE 1. SPIM parameters

R_{sd}: 0.473 Ω	Rated power: 1.1 kW
R_{sq}: 6.274 Ω	Rated voltage: 220 V
R_r: 5.514 Ω	Rated current: 5.1 A
L_{sd}: 0.0904 H	Rated frequency: 50 Hz
L_{sq}: 0.1099 H	Number of pole pairs: 2
L_r: 0.0904 H	Rated speed: 1430 rpm
M_{srd}: 0.0817	J: 0.9×10^{-3} kg·m^2
M_{srq}: 0.0715	f: 1.2×10^{-3} N·m·s·rad^{-1}

TABLE 2. PSMCs parameters

Parameters	Speed controller	Current controller
Switching factor	$C_w = 0.0001$	$C_{ids} = 0.01$, $C_{iqs} = 0.01$
Controller gain	$K_w = 50$	$K_{ids} = 150$, $K_{iqs} = 250$

4.2. **Results and interpretation.** Many experimental tests are realised to check out the effectiveness of the proposed IRFOC strategy and the dynamic performances of the designed SM controllers. The SPIM is subject to different scenarios of speed and load torque, where the reference rotor flux is kept constant at the nominal value 0.7 Wb. In such tests, the simulated and experimental waveforms of the SPIM speed, d-q rotor flux, d-q currents and switching functions are given simultaneously.

• Test 1: nominal speed (no load torque)

Initially, the SPIM is started up to nominal speed (1500 rpm) followed by an inversion of sign at 5 s and without load. The results show the quasi similarity between simulation and experimental behaviours. The rotor speed behaviours (Figure 4.1) express a good transient response (0.75 s), with a neglected steady error ($< 0.5\%$) and no relevant overshoot ($< 1\%$). Compared with the results obtained in [8], using the conventional PI regulators, a rapid response amelioration (about 25%) is noted. The direct and quadratic rotor flux waveforms (Figure 4.3) show that the rotor flux is totally aligned with the d-axis. Figure 4.2 demonstrates that the state variable (speed) reaches the desired SS in finite time ($t_{r\omega} = 0.65$ s) and remains there.

• Test 2: inversion of sign with load torque

In the second test, a step speed reference of 1000 rpm and a load torque equal to 4 N.m are applied to the SPIM via the magnetic powder brake followed by an inversion

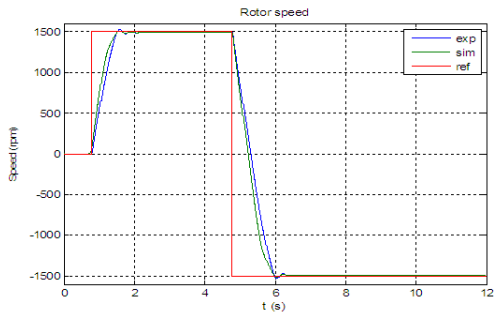

FIGURE 4.1 Rotor speed response

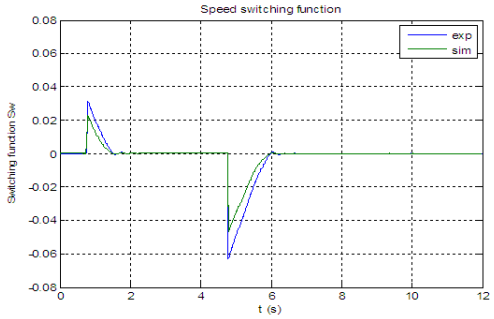

FIGURE 4.2 Speed switching function

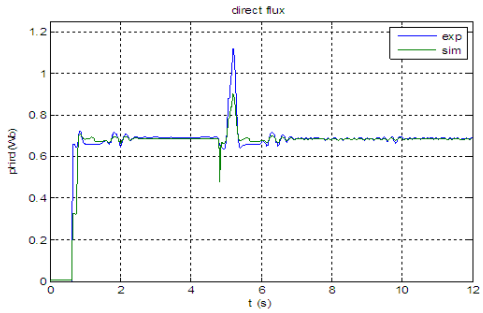

FIGURE 4.3.1 Direct flux waveform

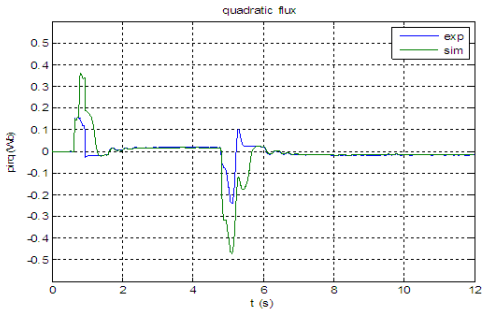

FIGURE 4.3.2 Quadratic flux waveform

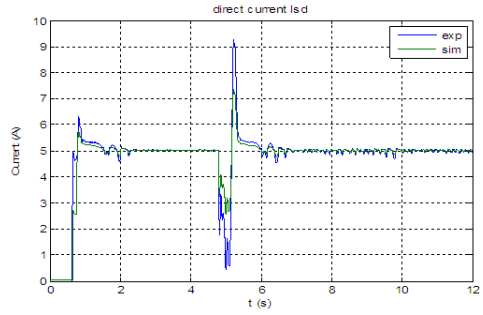

FIGURE 4.4.1 Direct current waveform

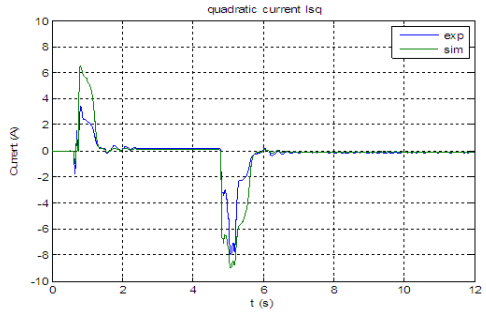

FIGURE 4.4.2 Quadratic current waveform

of sign at 7 s. The SPIM performances exhibit a good transient speed response and a good disturbances rejection (Figure 5.1). Then, the disturbances resulting from the load torque application have no relevant effect on the SPIM speed behaviour which stays inside the 0.5% error strip. The currents waveforms (Figure 5.4) prove obviously that the decoupled objective of the IRFOC strategy is achieved and so the direct and quadratic currents are controlled separately via the flux and the electromagnetic torque. Even with the presence of disturbances, the desired speed SS is reached and are maintained in finite time ($t_{r\omega} = 0.5$ s). This proved the robustness of the designed control law against external disturbances.

• Test 3: low speed with load torque

The last test was made to check the performances of the SM controllers in the low speed range. So, a step speed reference of 300 rpm with the same load torque is applied to the SPIM followed by an inversion of sign at 6 s. Figure 6.1 gives the speed behaviour which remains acceptable and not affected by the load torque insertion.

The speed SS (Figure 6.2) is also reached in finite time. The obtained speed reaching time is inferior to the one obtained in the second test, which is in concordance with the Equation (41). Figure 6.4 shows that the direct and quadratic currents oscillate around their desired values. Despite the notated currents oscillations, Figure 6.3 indicates that

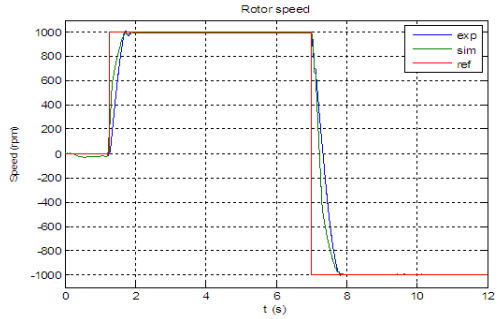

FIGURE 5.1 Rotor speed response (with load torque)

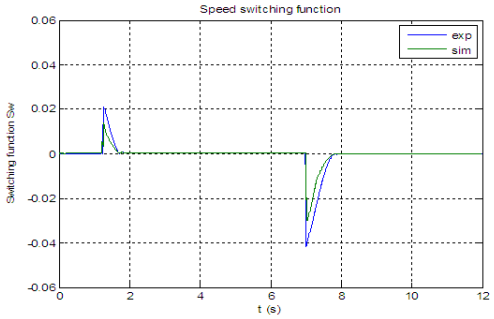

FIGURE 5.2 Speed switching function

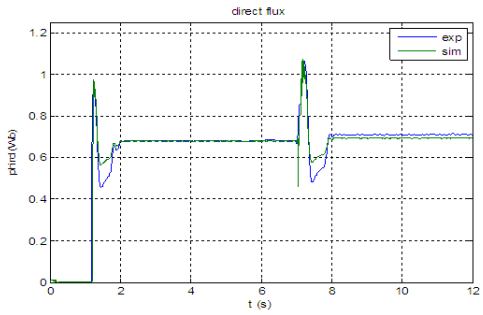

FIGURE 5.3.1 Direct flux waveform

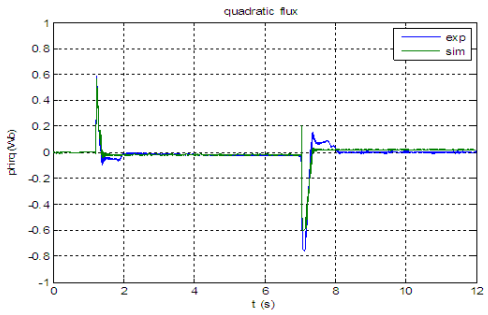

FIGURE 5.3.2 Quadratic flux waveform

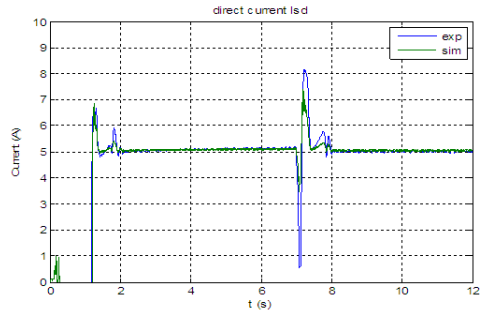

FIGURE 5.4.1 Direct current waveform

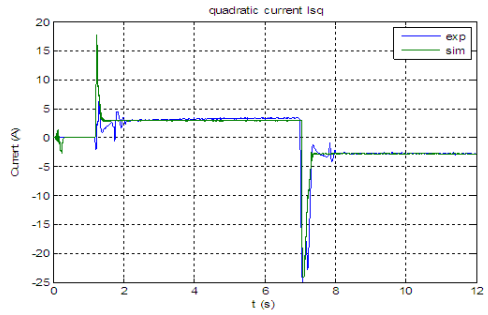

FIGURE 5.4.2 Quadratic current waveform

the direct and quadratic rotor flux attain their references and that the decoupled objective is maintained even at low speed range.

5. **Conclusion.** A novel IRFOC approach to drive the speed of two windings SPIM based PSMC was proposed. The originality was the removal of the decoupling bloc, usually required to implement the IRFOC method with the conventional controllers. This purpose was achieved using the SMC technique based on a very simple sliding surface design. Furthermore, the adoption of adaptive sliding gain within the approximation of signum function by smoother continuous one enables us to reduce the chattering effects for real time DSP implementation. After developing the theoretical aspects of the proposed IRFOC strategy, the entire control scheme of the SPIM drive including the design of three PSMCs was analyzed. As well, the stability of the designed PSMCs was proved using the Lyapunov theory. In order to investigate the validity of the whole proposed IRFOC strategy, an experimental platform was built. This platform was conceived around: a digital signal processor board dSPACE DS 1104, three-leg voltage source inverter and a commercial squirrel-cage SPIM. The simulation and experimental results obtained via several tests exhibit high-dynamic performances and guarantee a good rejection of external torque disturbances. So, both the speed and stator current reach their references without

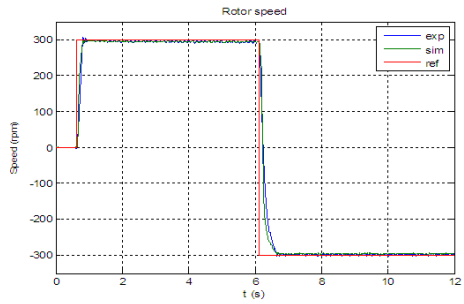

FIGURE 6.1 Rotor speed response (very low range)

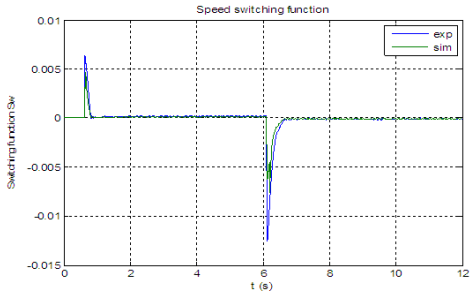

FIGURE 6.2 Speed switching function

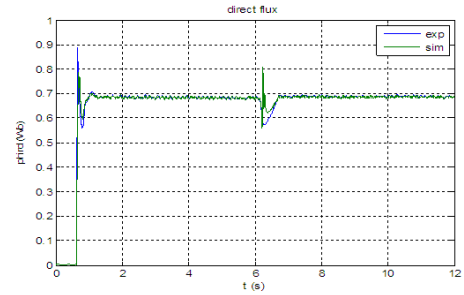

FIGURE 6.3.1 Direct flux waveform

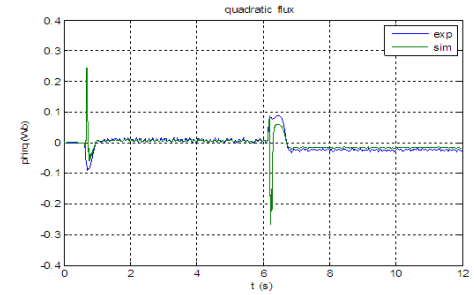

FIGURE 6.3.2 Quadratic flux wave form

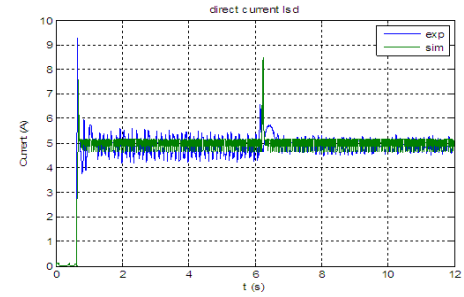

FIGURE 6.4.1 Direct current waveform

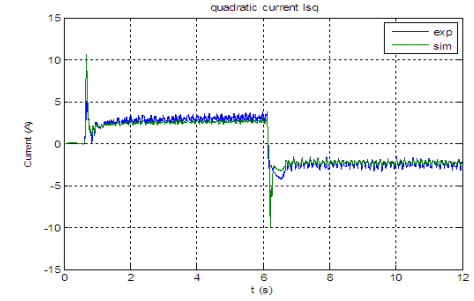

FIGURE 6.4.2 Quadratic current waveform

Nomenclature

- $v_{s\alpha}$, $v_{s\beta}/v_{sd}$, v_{sq}: stator voltages in stationary/synchronous reference frame;
- $i_{s\alpha}$, $i_{s\beta}/i_{sd}$, i_{sq}: stator currents in stationary/synchronous reference frame;
- $\varphi_{s\alpha}$, $\varphi_{s\beta}$: stator fluxes in stationary reference frame;
- $i_{r\alpha}$, $i_{r\beta}$: rotor currents in stationary reference frame;
- $\varphi_{r\alpha}$, $\varphi_{r\beta}/\varphi_{rd}$, φ_{rq}: rotor fluxes in stationary/synchronous reference frame;
- L_{sd}, L_{sq}, L_r, M_{srd}, M_{srq}: stator and rotor self and mutual inductances;
- R_{sd}, R_{sq}, and R_r: stator and rotor resistances;
- ω_r, ω_{sl}: rotor angular frequency, slip angular frequency;
- T_e, T_L: electromagnetic and load torque;
- f: friction coefficient;
- J: total inertia;
- n_p: pole pairs number;
- p: Laplace operator;
- V: candidate Lyapunov function;
- S_ω, S_d, S_q: Speed, direct current, quadratic current switching function;
- c_ω, c_d, c_q: Speed, direct current, quadratic current switching function factor;
- K_ω, K_d, K_q: Speed, direct current, quadratic current sliding gain;
- $t_{r\omega}$, t_{rd}, t_{rq}: Speed, direct current, quadratic current reaching time;
- U_{eq}: equivalent control law;
- U_d: non-linear control law;
- sign: signum function.

relevant damping or overshoot under loaded or unloaded conditions. In addition, the developed speed PSMC depends only on the engineer parameters choice. Therefore, they operate in robust mode against eventual motor parameters variation. A sensor-less speed controller using the sliding mode technique will be a natural perspective of this work.

REFERENCES

[1] J. R. Wells, B. M. Nee, M. Amrhein, P. T. Krein and P. L. Chapman, Low-cost single-phase powered induction machine drive for residential applications, *The 9th Annual IEEE Applied Power Electronics Conference and Exposition*, vol.3, pp.1579-1583, 2004.

[2] T. Fleiter, W. Eichhammer and J. Schleich, Energy efficiency in electric motor systems: Technical potentials and policy approaches for developing countries, development policy, statistics and research branch, *Working Paper 11/2011*, United Nations Industrial Development Organization, Vienna, 2011.

[3] B. Zahedi and S. Vaez-Zadeh, Efficiency optimization control of single-phase induction motor drives, *IEEE Transactions on Power Electronics*, vol.24, no.4, 2009.

[4] S. Reicy and S. Vaez-Zadeh, Vector control of single-phase induction machine with maximum torque operation, *IEEE ISIE*, Dubrovnik, Croatia, pp.923-928, 2005.

[5] R. Saidura, S. Mekhilef, M. B. Ali, A. Safari and H. A. Mohammed, Applications of variable speed drive (VSD) in electrical motors energy savings, *Renewable and Sustainable Energy Reviews*, vol.16, pp.543-550, 2012.

[6] M. Thirugnanasambandama, M. Hasanuzzaman, R. Saidur, M. B. Ali, S. Rajakarunakaran, D. Devaraj and N. A. Rahimc, Analysis of electrical motors load factors and energy savings in an Indian cement industry, *Energy*, vol.36, pp.4307-4314, 2011.

[7] R. Saidur and T. Mahlia, Impacts of energy efficiency standard on motor energy savings and emission reductions, *Clean Technology and Environmental Policy*, vol.13, no.1, pp.103-109, 2011.

[8] M. Jemli, H. B. Azza and M. Gossa, Real-time implementation of IRFOC for single-phase induction motor drive using dSPACE DS 1104 control board, *Simulation Modeling Practice and Theory*, vol.17 pp.1071-1080, 2009.

[9] R. S. Kumar, K. V. Kumar and Dr. K. Ray, Sliding mode control of induction motor using simulation approach, *International Journal of Computer Science and Network Security*, vol.9, no.10, 2009.

[10] M. Jemli, H. B. Azza, M. Boussak and M. Gossa, Sensorless indirect stator field orientation speed control for single-phase induction motor drive, *IEEE Transactions on Power Electronics*, vol.24, no.6, 2009.

[11] M. B. R. Corrêa, C. B. Jacobina, A. M. N. Lima and E. R. C. da Silva, Rotor flux oriented control of a single phase induction motor drive, *IEEE Transactions on Industrial Electronics*, vol.47, no.4, pp.832-841, 2000.

[12] M. B. de R. Corrêa, C. B. Jacobina, E. R. C. da Silva and A. M. N. Lima, Vector control strategies for single-phase induction motor drive systems, *IEEE Transactions on Industrial Electronics*, vol.51, no.5, pp.1073-1080, 2004.

[13] M. Guerreiro, D. Foito and A. Cordeiro, A speed controller for a two-winding induction motor based on diametrical inversion, *IEEE Transactions on Industrial Electronics*, vol.57, no.1, 2010.

[14] S. C. Tan, Y. M. Lai and C. K. Tse, General design issues of sliding-mode controllers in DC-DC Converters, *IEEE Transactions on Industrial Electronics*, vol.55, no.3, 2008.

[15] C.-Y. Chen, Sliding mode controller design of induction motor based on space-vector pulse width modulation method, *International Journal of Innovative Computing, Information and Control*, vol.5, no.10(B), pp.3603-3614, 2009.

[16] K. B. Mohanty, development of fuzzy sliding mode controller for decoupled induction motor drive, *PARITANTRA*, vol.8, no.1, pp.33-39, 2003.

[17] J. Y. Hung, W. Gao and J. C. Hung, Variable structure control: A survey, *IEEE Transactions on Industrial Electronics*, vol.40, no.1, 1993.

[18] M.-L. Tseng and M.-S. Chen, Chattering reduction of sliding mode control by low pass filtering the control signal, *Asian Journal of Control*, vol.12, no.3, pp.392-398, 2010.

[19] K. D. Young, V. I. Utkin and U. Ozguner, A control engineer's guide to sliding mode control, *IEEE Transactions on Control Systems Technology*, vol.7, no.3, pp.328-342, 1999.

[20] M. Dal and R. Teodorescu, Sliding mode controller gain adaptation and chattering reduction techniques for DSP based PM DC motor drives, *Turk. J. Elec. Eng. & Comp. Sci.*, vol.19, no.4, pp.531-549, 2011.

[21] Q. P. Ha, H. Trinh, H. T. Nguyen and H. D. Tuan, Dynamic output feedback sliding-mode control using pole placement and linear functional observers, *IEEE Transactions on Industrial Electronics*, vol.50, no.5, 2003.